



A benchmark preview of liver vessel enhancement algorithms

Jonas Lamy, Odysée Merveille, Bertrand Kerautret, Nicolas Passat, Antoine Vacavant

► **To cite this version:**

Jonas Lamy, Odysée Merveille, Bertrand Kerautret, Nicolas Passat, Antoine Vacavant. A benchmark preview of liver vessel enhancement algorithms. Virtual Physiological Human (VPH), 2020, Paris, France. hal-02537816

HAL Id: hal-02537816

<https://hal.archives-ouvertes.fr/hal-02537816>

Submitted on 9 Apr 2020

HAL is a multi-disciplinary open access archive for the deposit and dissemination of scientific research documents, whether they are published or not. The documents may come from teaching and research institutions in France or abroad, or from public or private research centers.

L'archive ouverte pluridisciplinaire **HAL**, est destinée au dépôt et à la diffusion de documents scientifiques de niveau recherche, publiés ou non, émanant des établissements d'enseignement et de recherche français ou étrangers, des laboratoires publics ou privés.

A Benchmark Preview of Liver Vessel Enhancement Algorithms

Jonas Lamy^{a*}, Odyssee Merveille^b, Bertrand Kerautret^a, Nicolas Passat^c, Antoine Vacavant^d

^a *Université Lyon 2, LIRIS (UMR 5205) Lyon, France*

^b *INSA de Lyon, CREATIS (UMR 5220) Lyon, Villeurbanne, France*

^d *Université de Reims Champagne Ardenne, CReSTIC, EA 3804, 51097 Reims, France*

^c *Université Clermont Auvergne, CNRS, SIGMA Clermont, Institut Pascal, F-63000, Clermont-Ferrand, France*

Keywords Liver, Vessels, Benchmark, Filtering, Computed Tomography, Magnetic Resonance Imaging

1. Introduction

Blood vessel segmentation has been a widely covered topic in the literature, in particular regarding retinal, brain and heart vascular networks. A renewed interest has been observed recently, in hepatic vessels extraction to develop computer-aided diagnosis and surgery planning tools. A good knowledge of the hepatic vascular network geometry is crucial for liver resection as the location of the main hepatic vessels helps the clinicians to determine the part of the liver to remove. Most segmentation algorithms include a filtering step that enhances the contrast of blood vessels while removing non-vessel structures in the image.

In the past twenty years, several vessel enhancement filters have been proposed. However, the implementations used in the published articles have rarely been made publicly available, and the quantitative analyses have often been performed on a limited number of methods on homemade synthetic examples and/or private datasets of real images. The reproducibility and comparison of the results from the different methods are thus very difficult.

In this work, we implemented seven vessel enhancement filters representative of the literature and compared their results. This benchmark is established on two publicly available datasets: (i) the *IRCAD* dataset containing 20 Computed Tomography (CT) scans of patients and (ii) a synthetic dataset from *VascuSynth* [4] corrupted by noise and photometric artifacts.

2. Methods

2.1 Vessel enhancement filters

The first category of filters studied in this work, called *vesselness*, is based on the analysis of the Hessian matrix for each voxel. Let $\lambda_1, \lambda_2, \lambda_3$ be the eigenvalues of the Hessian matrix such that $|\lambda_1| \leq |\lambda_2| \leq |\lambda_3|$; then a tubular structure can be described by:

$$|\lambda_1| \approx 0; \quad |\lambda_1| \leq |\lambda_2|; \quad \lambda_2 \approx \lambda_3 \quad (1)$$

Vesselness filters define a ratio of eigenvalues to

discriminate tubes from other structures. Most vessel enhancement filters in the literature are vesselness filters. Five of them were selected to represent this category: Sato [8], Frangi [1], Meijering [2], Jerman [7] and Zhang [6]. These filters are coupled with a Gaussian scale-space framework to detect vessels of varying size. In this framework, the scale parameter is then defined as the standard deviation σ of the Gaussian.

Two non-vesselness methods were also selected. The first is the Optimally Oriented Flux (OOF) which is an optimization framework leading to the computation of 3 eigenvalues. These values play the same role as those of the Hessian matrix, while avoiding some drawbacks caused by the scale space. We use the OOF framework with the vesselness measure [3]. The second method, called RORPO [5], is based on path operators, from mathematical morphology, that uses path-based structuring elements to detect curvilinear structures. RORPO is also a multiscale filter using the length of the structuring elements as the scale parameter.

2.2 Dataset and implementation

The *IRCAD* dataset contains 20 CT scans of the liver along with their vascular network ground-truth. The *VascuSynth* dataset from March 2013 contains 11 groups of 10 synthetic vascular networks with a varying number of bifurcations. Noise was added to the *VascuSynth* dataset to simulate either CT (combination of Poisson and Gaussian noise) or Dynamic Contrast-Enhanced Magnetic Resonance (DCE MRI) acquisition (non-linear illumination and Rician noise).

The implementation of the seven compared methods is proposed in a common framework publicly available on *GitHub* (<https://github.com/JonasLamy/LiverVesselness>). The scripts to generate the results and analysis presented below are also available.

2.3 Metrics

Each filter provides a normalized response acting as an indicator to belong to a blood vessel ranging from 0 to 1. To assess the efficiency of the seven algorithms, the results were thresholded iteratively from 0 to 1. Each resulting binary image was compared to the vascular network ground-truth to compute the

*Corresponding author. Email: jonas.lamy@univ-lyon2.fr

number of true positives, true negatives, false positives and false negatives. Three similarity criteria were computed from these values: the Matthews correlation (MCC), the Dice coefficient and the minimum distance to the point (0 FP, 1 TP) of the ROC curve.

3. Results and discussion

In this work, each method was computed on half images of both datasets. Illumination artifacts and Rician noise ($\sigma = 20$) were added to the *VascuSynth* samples. The parameters for each filter were independently optimized in two steps: First, the best set of scales was determined while the other parameters were set to their default value, then the specific method parameters were optimized using the best set of scales. As the results may depend on the chosen metric, we repeated this optimization process with a grid search based on each metric.

We observed that the MCC tends to penalize false positives which results in a smaller range of scales centered on large scales to detect large, better contrasted vessels. We also observed that the MCC and Dice values are highly correlated, as such we will only comment one of them. The distance to the ROC curve seems to encourage a high true positive rate resulting in a wider range of scales.

On real data, most false positives from the Frangi, Jerman, Sato, Meijering, OOF and Zhang filters are located on the liver border whereas RORPO does not detect false positives on the liver border.

For the *IRCAD* database Zhang's algorithm provides the best results closely followed by Sato's and Frangi's. For the *VascuSynth* dataset, Sato gives the best metrics followed by Jerman and Frangi. The quantitative results for both experiments are shown in Table 1 and the best ROC curves for each method on the *IRCAD* dataset are presented in Figure 1.

This benchmark will be extended to DCE-MRI images to better assess the behavior of vessel enhancement filters on this specific modality.

Specific metric to assess the quality of the bifurcation detection will be included in this benchmark as it is often a weak point of vessels enhancement algorithms.

DataBase	<i>VascuSynth</i>			<i>IRCAD</i>		
	MCC	Dice	dist	MCC	Dice	dist
Sato	0.846	0.842	0.052	0.345	0.360	0.349
Frangi	0.830	0.828	0.055	0.340	0.355	0.365
Meijering	0.656	0.637	0.111	0.178	0.188	0.440
OOF($\lambda_1 + \lambda_2$)	0.510	0.500	0.143	0.240	0.240	0.456
Jerman	0.837	0.833	0.054	0.322	0.330	0.368
RORPO	0.420	0.350	0.411	0.292	0.284	0.748
Zhang	0.767	0.760	0.100	0.392	0.398	0.347

Table 1: Comparison results obtained on the *VascuSynth* and *IRCAD* database.

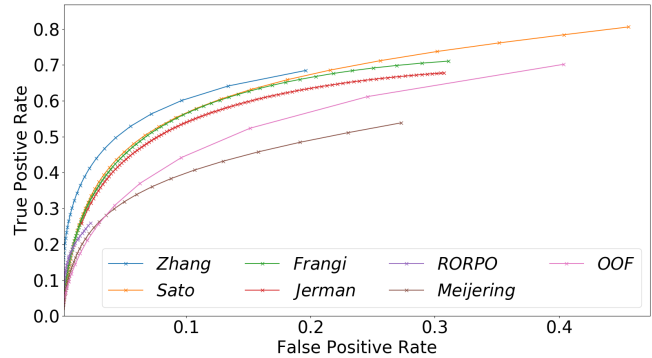


Figure 1: ROC curve after maximizing MCC for the *IRCAD* database.

4. Acknowledgements

This work was funded by the French *Agence Nationale de la Recherche* (R-Vessel-X, grant ANR-18-CE45-0018).

5. References

- [1] A.F. Frangi *et al.* Multiscale vessel enhancement filtering. In *MICCAI*, pages 130–137, 1998.
- [2] E. Meijering *et al.* Design and validation of a tool for neurite tracing and analysis in fluorescence microscopy images. *Cytometry*, 58A:167–176, 2004.
- [3] F. Benmansour *et al.* Tubular structure segmentation based on minimal path method and anisotropic enhancement. *Int J Comput Vision*, 92:192–210, 2011.
- [4] G. Hamarneh *et al.* Vascusynth: Simulating vascular trees for generating volumetric image data with ground-truth segmentation and tree analysis. *Comput Med Imag Grap*, 34:605–616, 2010.
- [5] O. Merveille *et al.* Curvilinear structure analysis by ranking the orientation responses of path operators. *IEEE T Pattern Anal*, 40:304–317.
- [6] R. Zhang *et al.* An improved fuzzy connectedness method for automatic three-dimensional liver vessel segmentation in CT images. *J Healthc Eng*, 2018:1–18, 2018.
- [7] T. Jerman *et al.* Beyond Frangi: An improved multi-scale vesselness filter. In *Medical Imaging: Image Processing*, volume 9413, page 94132A, 2015.
- [8] Y. Sato *et al.* 3d multi-scale line filter for segmentation and visualization of curvilinear structures in medical images. In *CVRMed-MRCAS*, pages 213–222, 1997.